MICROPLASTICS TRANSPORT AND MIXING MECHANISMS IN THE NEARSHORE REGION

Soroush Abolfathi[1], Sarah Cook[2], Abbas Yeganeh-Bakhtiary[3], Sina Borzooei[4] and Jonathan Pearson[1]

Microplastics (MP) are emerging pollutants in the marine environment with potential ecotoxicological effects on littoral and coastal ecosystems. A dominate contributing source of microplastic particles is the fragmentation of macroplastics from manufactured goods, alongside laundered synthetic material, abrasion of vehicle tyres and personal care products. The indiscriminate use of plastic and poor management of plastic waste pose serious threat to ecosystem functionality and resilience. Understanding the key underlying transport and mixing mechanisms which influence the behavior of microplastics and their environmental fate are crucial for identify potential microplastic fate-transport pathways from source to sink. This is fundamental for evaluating microplastic interactions and impact on ecosystems. This paper presents laboratory-based tracer measurements for solute and polyethylene (PE) microplastics in the presence of waves. The tests were undertaken in a wave tank equipped with an active absorption paddle-type wave-maker. Fluorescent dye was used to stain the PE particles using a novel staining technique. Rhodamine dye was used as a proxy for the transport of solute pollutants. The temporal and spatial behavior of both microplastics and solute across the nearshore zone was measured using submersible fiber optic fluorometers. Hydrodynamic conditions were designed to create monochromatic waves with a range of wave steepness $S_{op} = 2 - 5$ %. Tracer measurements were conducted at three locations, seaward of the breaker region, breaker region and inner surf zone to provide a comprehensive understanding of mixing across the nearshore. The dispersion coefficients were determined for both solute and PE particles. The results indicate the dominant role of surface and bed generated turbulence in determining mixing and dispersion influenced by wave breaker type and width of the surf zone. The comparison of tracer data suggests that PE particles, with similar density to water, and the solute tracer have a similar transport and mixing behavior under the influence of waves.

Keywords: microplastics; nearshore; turbulent mixing; dispersion; pollution transport; fluorometric tracing

INTRODUCTION

Nearshore zone experiences pollutant loading through both the shoreline and seaward boundaries. From the seaward boundary, pollutant loading is transported landward towards the surf zone by the so-called Stokes drift effect (Stokes, 1847). From the shoreline boundary, runoff pollution, which can contain faecal indicator bacteria and human viruses (Abolfathi and Pearson, 2014 and 2017) can drain into the surf zone. Consequently, pollution can accumulate in the nearshore region, and as such, the water quality can affect the health of the general public, visting coastal regions, representing a global problem. Yet, the key mass exchange processes related to the pollutant transport and dilution, within the nearshore water body, reamin poorly understood.

Microplastics (MP) pollution in the nearshore and coastal waters is an emerging global environmental problem (Jambeck et al., 2015). Microplastics are defined as plastic particles with the largest dimension smaller than 5 mm. MPs are composed of different polymer types with heterogeneric behaviour in aquatic flow based on their differing physical properties, including density, geometrical shape and particle size. They can originate from primary sources (i.e. abrasive microbeads in cosmetics and cleaning products) specifically manufactured within that micrometre range, alongside secondary sources, whereby larger plastic items (i.e. plastic bottles) are fragemented into smaller particle sizes from physical, chemical and biological degradation. These degradation processes often include exposure to UV radiation, mechanical abrasion from wave and wind action and biodegradation (Wright and Kelly, 2017).

The transport and fate of microplastics in the nearshore environment is predominantly influenced by surface-generated turbulence due to wave breaking processes. This is combined with the vertical and transverse structure of shear flow from complex three-dimensional flow fields resulteing from wave-current interactions. The sediment transport and erosion-deposition processes influenced by nearshore hydrodynamics (Fitri et al., 2019; Yeganeh-Bakhtiary et al., 2020) also play important role in the dynamic interactions between pollutants (e.g., microplastics) and nearshore processes. The interplay between microplastics, sediment bed, bacteria and viruses can also form biofilms on microplastics and alter their physical properties (e.g., density). This can lead into changes in the mixing and transport of microplastics across the nearshore and their hyporheic exchange (Cook et al., 2020b). Identifying the key

[1] School of Engineering, University of Warwick, CV4 7AL, Coventry, United Kingdom
[2] School of Biosciences, University of Nottingham, Loughborough, LE12 5RD, UK
[3] School of Civil Engineering, Iran University of Science and Technology, 16844, Tehran, Iran
[4] Department of Civil and Environmental Engineering, Politecnico di Torino, 10129, Torino, Italy

physical driving mechanisms of mixing and transport for microplastics of varying size, shape and density within dynamic nearshore region, and quantifying these mechanisms for different types of microplastics is necessary for understanding the fate, environmental impacts and potential for ecotoxicity of microplastics within the marine environment.

EXPERIMENTAL METHOD

This paper presents an experimental investigation to understand and quantify the key underlying transport mechanisms of a very common type of microplastics, Polyethylene (PE), under the influence of wave actions. PE is the most abundant synthetic polymer found in water bodies (Lebreton et al., 2017). This is mainly due to the fact that PE is generally used for packaging material, predominately for single use products (i.e. plastic bags, plastic films, etc.). Also, some studies suggest that PE can be a vector for organic contaminants and pathogens through absorption (Seidensticker et al., 2018) highlighting the urgent need for understanding transport and dispersion mechnaisms for PE microplastics.

A novel integrated fluorometric measurement system is developed to measure the combined dispersive and diffusive processes at various locations across the nearshore. The fluorometric properties were added to PE microplastic particles using a microplastic staining technique developed at Warwick Water (Cook et al., 2020a).

Hydrodynamics and Fluorometric measurements were conducted in a flume of 20m (L) x 0.6m (W) x 1m (H), with a smooth 1:20 foreshore beach slope. Three monochromatic wave conditions with varying steepness, $S_{op} = 2 – 5\%$, were used to represent the typical wave conditions across Europe. Waves were generated using a paddle-type wavemaker equipped with an active-absorption system.

Wave surface elevations were measured using six gauges located near the paddle (offshore region) and within the inner surf zone. The location of the wave gauges was determined following Mansard and Funke's (1980) methodology. The wave gauge data was used to understand both incident and reflected wave characteristics across the nearshore, using a least squares method (Dong et al., 2018 and 2020; Salauddin et al., 2020). Figure 1 illustrates a schematic of the experimental setup. To compare the behavior of microplastics with the solute dispersion, tracer measurements with Rhodamine Water Tracing dye were conducted for all the wave conditions. The tracer signals from PE microplastics and Rhodamine were compared to better understand the behavior of microplastics particles with a density similar to the density of water. In order to provide a comprehensive dataset on the behaviour and dispersion of PE and solute across the nearshore region, the tracer tests were conducted in three locations including seaward of the bearker region, breaker region and inner surf zone.
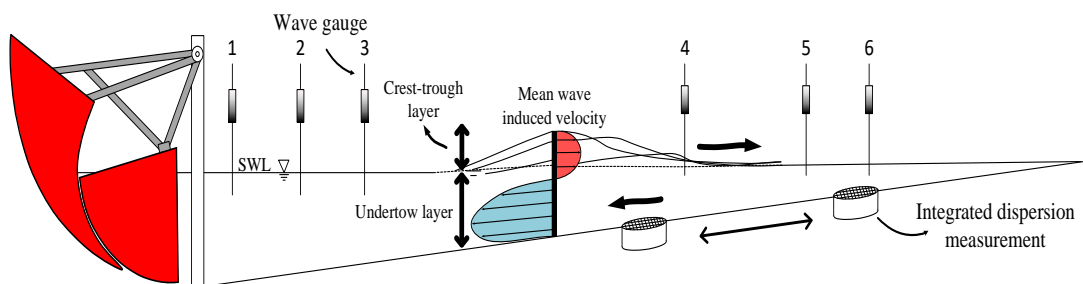

Figure 1. Schematic of experimental setup

Wave Conditions

This study mainly focuses on monochromatic waves with the wave steepness of 2 – 5% which is the typical wave steepness across the Europe. The offshore wave height, near the paddle, was kept constant across all the wave conditions with varying wave period of 1.2, 1.85 and 2.2 seconds. Table 1 summarizes the wave conditions measured in this study.

The wave surface elevation in the offshore region and across the nearshore were measured using six wave gauges. The wave conditions were logged continously for the duration of both Rhodamine and PE

tracer tests. The characteristics of incident and reflected waves were determined using reflection analysis method outlined in Mansard and Funke (1980).

Table 1. Measured wave conditions in the offshore region (near the paddle).

Nominal wave steepness (S_{op})	Offshore wave height H_o [m]	Offshore wave period T_p [s]	Offshore wave steepness S_{op} [%]
5.0%	0.122	1.20	5.49
3.5%	0.121	1.85	3.55
2.0%	0.119	2.90	2.08

Figure 2 shows the wave height measurements across the nearshore for all the wave conditions tested in this study. Figure 2 indicates that for all the tested conditions, the breaker region is approximately 3 m from the still water line (SWL).
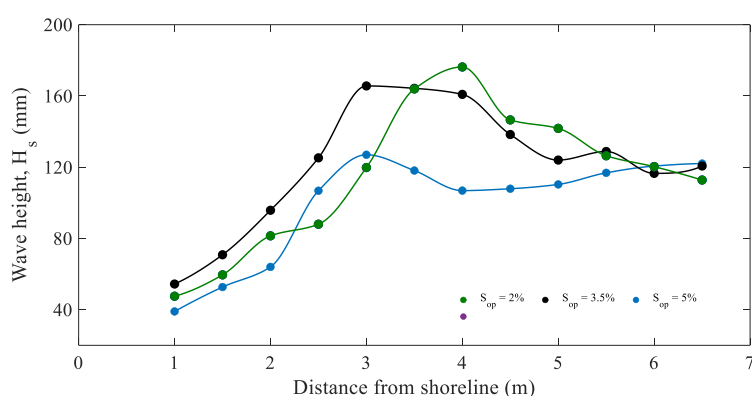

Figure 2. Wave height measurements across the nearshore for all the wave conditions.

Microplastic Staining Technique

Polyethylene (PE) microplastic particles with the density of 0.975 g/cm^3 were used for MP tracer tests in this study. The relatively low density of PE allows for neutrally buoyant behaviour of MP particles within water column. The tracer tests were undertaken with spherical PE powder with a diameter of 40-46 µm. The PE staining method incorporated three incubation cycles of PE and Nile Red (NR) within a water bath to allow for the diffusion of dye molecules into the hydrophobic environment of the microplastic material (Karakolis et al., 2019). The NR (technical grade, N3013, Sigma-Aldrich) dye was created to a working solution of 100 µg ml^{-1} by dissolving 10 mg of NR in 100 ml of methanol, following the methodology outlined in Cook et al. (2020a). This process involved mixing of PE powder (4 grams) with 80 ml of dimethyl sulfoxide and ultrapure water (v=1:1) solution in a 100 ml lid sealed beaker. The suspended MPs were then incubated at room temperature (25°C), 50°C and 75°C for a period of 10, 20 and 30 minutes, respectively. Before each incubation, 8 ml of NR was added to the solution. After the final incubation, the plastic content was filtered and rinsed with deionised water until the filtrate ran clear (Cook et al., 2020a). following a 48 hours drying period, the MPs were stored in dark containers to limit the degradation of microplastic fluorescence.

Weight measurements of stained MPs were taken after the NR staining process. It was found that the total weight of the particles slightly increased after the staining process, however the majority of this increase weight can be related to MPs particle's saturation with de-ionised water at the time. No weight measurements were conducted after the aerating process. The analysis of PE tracing restuls show that the potential weight, and therefore density increase is minimal and the particles remain neutrally buoyant in the water column.

Fluorescence Tracer Sensors

Turner Design Cyclops-7 and Cyclops-7f sensors are submersible fiber optic fluorescence detectors, capable of detecting fluorescent particles up to 15cm. The tracer tests were undertaken with three Cyclps-7 fluorometer fixed at three on-offshore locations of 1, 3 and 5m from SWL. The tracer measurement

sensors were fixed at mid-depth of the still water column at each on-offshore location. The sesonrs were mounted from a fixed frame at an angle of 20° to ensure maximum detection of the tracer cloud. The concentration of fluorescent particles were reocrded constantly throughout the experiments at 0.5 s time intervals. The fluorescent particles (Rhodamine and PE), were detected by fiber optic sensors as increased voltage in the recorded data. Following calibrations, the voltage values recorded by Cyclops were converted to concentration values for Rhodamine [ppb] and MP [mgL^{-1}] using linear calibration curves ($R^2 \geq 0.9824$).

Individual calibrations were completed for all of the fiber optic fluorometer sensors, for both Rhodamine and MP. The calibration process was conducted in individual bucket containers filled with 10 L of 15°C water, to minimize the inaccuracy of calibration due to the interaction between sensors. For the calibration tests, Rhodamine (106 ppb) and PE were injected into the container in measurements of 50 µl, using a micro-adjustable pipette, and 40 mg, using a small vial filled with 10ml of water, respectively.

Following the tracer injection to calibration set, the water was thoroughly mixed in such a way to avoid the creation of a whirlpool that would concentrate the location of the tracer at the centre of the container. This process was repeated until the total concentration of Rhodamine and MP within their respective containers had reached 250 µl and 240 mg, respectively.

Table 2. Rhodamine and PE Calibration values for fluorometer sensors.

Tracer		Sensor (1)	Sensor (2)	Sensor (3)	Sensor (4)	Sensor (5)
	Gradient	49.619	58.330	57.394	60.795	57.184
Rhodamine	Intercept	-3.3782	-2.543	-4.2019	-1.6158	-0.7214
	R^2 Value	0.9858	0.9993	0.9924	0.9972	0.9994
	Gradient	73.071	148.620	58.525	133.550	108.150
Microplastics	Intercept	-3.2049	-6.0142	-1.6472	-2.4983	-0.633
	R^2 Value	0.9824	0.9955	0.9824	0.9977	0.9913

The collected data from the calibrations will form discrete steps (see Figure 3a), that show the increase of voltage as tracer concentration is incrimentaly increased over a period of time. The sharp jump in the voltage level is related to when a new quantity of tracer was added to the calibration setup. Each step was then isolated, with an average of each step taken to determine the data points used for the linear calibration curve (Figure 3b). The data within each step showed a decrease in voltage over the 60 second settling period, implying that the peak concentration of the tracer was reached after being thoroughly mixed, similar to the turbulent wave actions within the experimental setup. The values acquired from the linear calibration curves are shown in Table 2.

Following the calibration process for both PE and Rhodamine WT dye, the tracers were injected in the offshore region of the wave tank, near the paddle, using manual pulse injections. The tracers were injected in the offshore boundaries of the flume to ensure the contaminant was well-mixed within the water column before reaching the nearshore region.

Data Processing

Following the tracer measurement tests, the background concentration was removed from the raw concentration data before proceeding to data analysis. The background concentration was defined as the mean concentration during the 1minute period before tracer injection. The data show that PE microplastic injections generated a more scattered dispersion band which was also reported by Cook et al. (2020a).
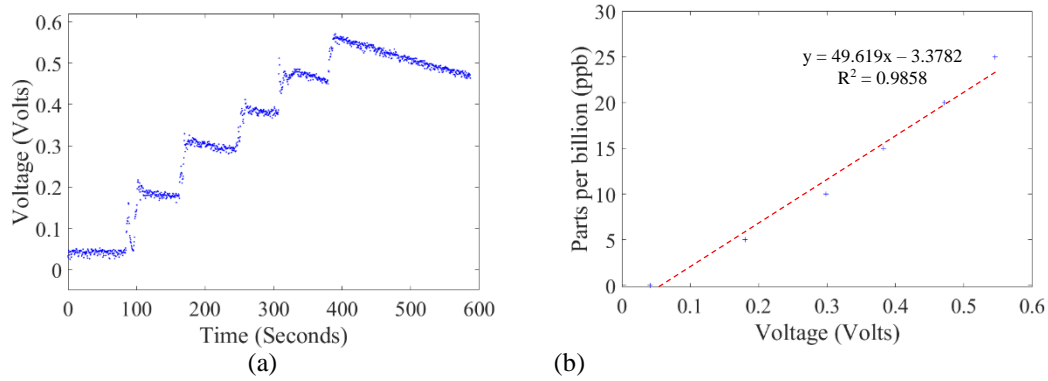
Figure 3. Typical fluorometer sensor calibration graphs: (a) Voltage vs Time, (b) Concentration vs Voltage.

Advective dispersion coefficients were determined from the temporal variation of concentration distribution across the three on-offshore locations in the nearshore region. The cut-off value of the distribution curve was defined as the point where the concentration at the tail of the curve reached approximately 5% of the peak concentration, following the methodology descibed by (Cook et al., 2020a; Abolfathi 2016; Abolfathi and Pearson, 2014). An interpolation line between the leading and end tails of the concentration distribution curves were used for eliminating the background concentration. Detailed analysis procedures for the tracer data are desribed in the 'Tracer Analysis' section of this paper.

THEORETICAL APPROACH

The mixing and dispersion of microplastics across the nearshore region (on-offshore direction) is dominated by broken wave-induced surface and bed generated turbulence varying in temporal and spatial scales. For shallow waters in the coastal area, following the assumption of wide beach with homogeneous velocity vectors [u(z) and v(z)] varying with depth (z) and not in spatial directions (x and y), the advective and diffusive processes that govern transport of solute and microplastics in two-dimensional Cartesian coordinate system can be described by Eq. 1:

$$\frac{\partial \bar{c}}{\partial t} + \bar{U}_i \frac{\partial \bar{c}}{\partial x_i} - \frac{1}{h} \frac{\partial}{\partial x_i}\left(d E_{i,j} \frac{\partial \bar{c}}{\partial x_i}\right) = -\frac{\bar{c}}{T_d} \tag{1}$$

where, i represents x in the on-offshore direction and j represents y, which is the longshore axis, d is the total depth of water, $\bar{U}_i$ is the depth-averaged velocity, $\bar{c}$ represents the depth-averaged mean concentration, T_d is the characteristic time-scale and $E_{i,j}$ is the depth-averaged diffusion-dispersion coefficient (Goodarzi et al., 2020a and b). Within the boundaries of the nearshore region, wave breaking is the dominant cause of transport and generates two strong mixing mechanisms due to the surface generated turbulence of the breaking wave, and the shear effects induced by the vertically non-uniform structure of the temporally-averaged flow (Abolfathi and Pearson, 2014 and 2017).

The mixing coefficient ($E_{i,j}$) in Eq. 1 incorporates both turbulent diffusion and advective shear dispersion and therefore, the mixing coefficient for microplastics can be written as:

$$E_{i,j} = \begin{cases} E_i = \nu_t + D_x \\ E_j = \nu_t + D_y \end{cases} \tag{2}$$

where, ν_t denotes the depth-averaged horizontal eddy viscosity, D is the advective shear dispersion in on-offshore (x) and longshore (y) directions. Following the methodology described by Taylor (1954) and Fischer et al. (1979), D can be described as a complex function of turbulent fluctuations (u') and vertical eddy viscosity (ν_z):

$$D = \frac{1}{d} \int_0^h u' \int_0^z \frac{1}{\nu_z} \int_0^z u' \, dz dz dz \tag{3}$$

The eddy diffusivities can be determined as a function of turbulent length-scale (l_m) and turbulent kinetic energy (k):

$$v_z = l_m . k^{1/2} \tag{4}$$

The total advective shear dispersion (D_x) for microplastics (with $\rho \cong \rho_w$) and solute in the nearshore can be defined as the sum of the dispersion due to non-uniform over the depth, secondary time-averaged on-offshore velocity profiles (D_s) and oscillatory wave motions (D_o). Literature shows that generally D_o is in the order of 0.1-0.6 v_t and therefore cannot play a significant role in dispersion (Abolfathi, 2016; Karambas, 1999). However, D_s mechanism, by incorporating dispersion due to mean opposite velocities in the shallow water column and non-uniform distribution of undertow is contributing to the overall mixing at a much larger scale. Abolfathi (2016) divided a well-mixed shallow water column to N zones of parallel flow moving with a depth-averaged velocity and fractional thickness of q (Figure 4), and developed coupled dispersion equations between two adjacent zones to determine the overall advective dispersion due to D_s at a particular on-offshore location, within nearshore environment, as a function of hydrodynamic structure over the water column. The overall system of PDEs was solved using Fourier transformation and large time exponent [$\gamma(\lambda)$] and overall shear dispersion can be written as Eq. 5:

$$
\begin{aligned}
D(\infty) = \lim_{N \to \infty} D(N) \\
= h^2 \int_0^1 \frac{q^2(1-q)^2}{Diff_y(q)} [u_b(q) - u_u(q)]^2 dq \\
+ \int_0^1 D_x(q) dq
\end{aligned}
\tag{5}
$$

where, $Diff_y$ is the diffusivities, u_b denotes the wave bore velocity and u_u is the undertow velocity. The laboratory measurements show that assumption of well-mixed microplastic over the shallow water column is correct and therefore Eq. 5 can be used to determine shear dispersion for PE microplastics when $\rho_{wmicroplastics} \cong \rho_{water}$. The overall mixing of PE microplastics and solute, in the on-offshore direction, is taken as the sum of Eq. 4 and Eq. 5.
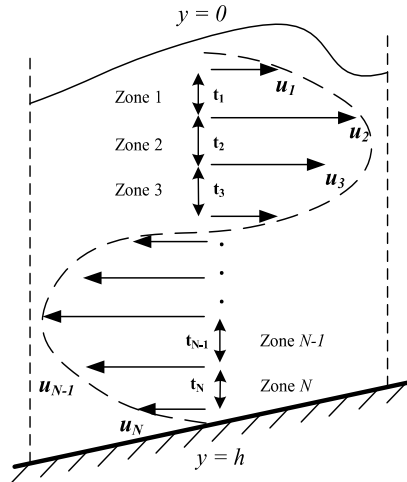

Figure 4. Definition sketch for *N* zone dispersion model in the nearshore region (Adopted from Abolfathi, 2016)

TRACER ANALYSIS

The behaviour of solute and microplastics in the nearshore region is investigated for a range of climate conditions including both swell and storm waves. For each hydrodynamic condition, the fluorometric studies were undertaken at three on-offshore locations to include offshore region (6 m from SWL), breaker region (3 m from SWL) and inner surf zone (2 m from SWL). Tracer measurements were

carried out at mid-depth of water column. PE microplastic particles were stained with Nile Red and used as tracer. Tracer injections for both PE and solute were carried out in the offshore region near the paddle.

The mixing coefficient from tracer data were determined using Fischer et al. (1979) which combines both diffusive and dispersive mixing mechanisms (Eq. 6).

$$c_d(x,y) = \frac{Q}{d\sqrt{4\pi D_y\, x u_d}} \exp\left(-\frac{y^2 u_d}{4D_y\, x}\right) \tag{6}$$

where, c_d is depth-averaged microplastic concentration, D_y is dispersion coefficient, u_d is longitudinal depth-averaged velocity and Q denotes the mass inflow rate of microplastic plume per unit width. Eq. 6 describes a Gaussian distribution shape for concentration, and the measure of spread about the bed can be quantified by spatial variance of distribution (σ^2) as:

$$\sigma_y^2 = \frac{\int_{-\infty}^{\infty}(y-\mu)^2 c_d(y)dy}{\int_{-\infty}^{\infty} c_d(y)dy} \tag{7}$$

The position of the centroid (μ) is determined as:

$$\mu = \frac{\int_{-\infty}^{\infty} y c_d(y)dy}{\int_{-\infty}^{\infty} c_d(y)dy} \tag{8}$$

Given that the spatial variance for Gaussian distribution increases linearly with the distance from the source (Abolfathi and Pearson, 2014), the mixing coefficient is measured in this study as the rate of change of variance:

$$D_y = \frac{u_d}{2}\frac{d\sigma_y^2}{dx} \tag{9}$$

Eq. 9 is adopted for analyzing both solute and microplastic tracer behaviour under different hydrodynamic conditions tested within this study.

RESULTS AND DISCUSSIONS

This paper presents laboratory investigations focused on understanding and quantifying the nearshore mixing processes for solute and PE microplastics due to the effects of waves. In the nearshore region, wave processes dominate the mixing and transport of pollutants due to the finite depth of water. Mixing under the influence of waves is dominated by wave-induced surface and bed generated turbulence across the nearshore and specifically inside the surf zone. The shear effects from the vertical and transverse variation of hydrodynamic structures in the shallow water column of the srufzone also play a key role in determining diffusive and dispersive mixing mechanisms in the nearshore region. Therefore, this study considered the total mixing coefficient as the sum of turbulent diffusion and advective shear dispersion (Eq. 2). The mixing coefficients from tracer data were determined with the methodology proposed by Fischer et al. (1979) which combines both diffusive and dispersive mixing mechanisms (Eq. 9). The tracer analyses were conducted with the assumption of solute and PE become vertically well-mixed within a short distance from the source (point source discharge). This is a valid assumption in the nearshore region where the water depth is relatively small compared to the flow width.

In order to reduce the complexity of considering and measuring all the associate parameters in the spreading of dye, the depth variation in the solute and PE concentrations can be ignored. Therefore, considering the variations of solute concentrations in the transverse and longitudinal directions, the depth-averaged mixing coefficient was determined in this study. Comparison of mixing coefficient between solute and PE microplastics, with similar density to density of water, can provide key information on how the transport and environmental fate of PE microplastics can be evaluated and modelled.

For all the tested hydrodynamic conditions, the response curves of the tracer injections were plotted as concentration (PE and Rhodamine) against time (Figure 5). The analysis of the travel times for PE and

Rhodamine WT dye concentration profiles suggest that both solute and MPs transport to the surf zone at similar rates.
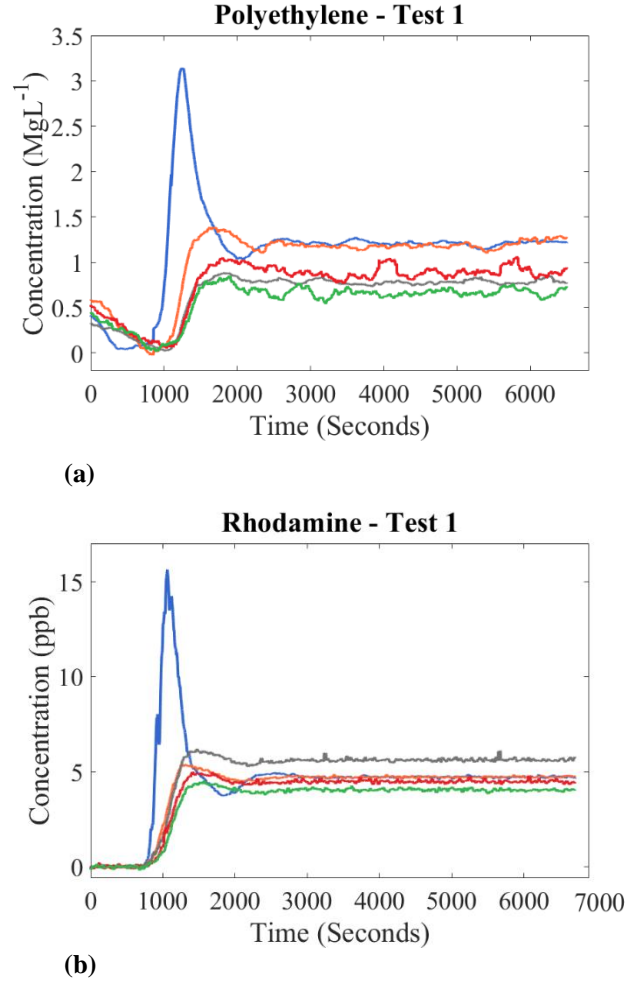
Polyethylene - Test 1

Rhodamine - Test 1

Figure 5. Temporal variation of tracer concentration at the breaker region: a) PE Microplasctis, and b) Rhodamine WT dye

Figure 5 shows the tracer measurements under monochromatic waves with an offshore wave height of 0.12m, wave period of 1.2 seconds and 5% wave steepness. The Figure compares the temporal variation of tracer behavior in the surf zone, highlighting the impact of surface and bed generated turbulence on the mixing of solute and microplastics. The mixing coefficient were determined from the tracer data using the method of Moment described by Eq. 6 – 9. Table 3 presents the mixing coefficient for all the tested wave conditions at the breaker region (= 3m from SWL).

Table 3. Dispersion coefficients at the breaker region (3m from SWL) for S_{op}=5%.

Nominal wave steepness (S_{op})	Offshore wave height H_o [m]	Offshore wave period T_p [s]	Longitudinal velocity U_d [m/s]	Bed shear velocity u_* [m/s]	Solute dispersion D_y [m²/s]	PE dispersion D_y [m²/s]
5.0%	0.122	1.20	0.15	0.0075	1.241×10^{-2}	5.604×10^{-3}
3.5%	0.121	1.85	0.15	0.0075	8.109×10^{-3}	2.620×10^{-3}
2.0%	0.119	2.90	0.15	0.0075	1.056×10^{-2}	2.417×10^{-3}

The comparison of mixing coefficients from PE microplastics and Rhodamine WT dye presented in Table 3 suggests similar transport and dispersion behaviour for both PE and solute which can be associated to comparable denisty of water and PE.

REFERENCES

Abolfathi, S., J. M. Pearson. 2014. Solute dispersion in the nearshore due to oblique waves. *Proceedings of 14th International Conference on Coastal Engineering*, ASCE, 1(34), waves 49. ISBN 9780989661126. ISSN 2156-1028. https://doi.org/10.9753/icce.v34.waves.49.

Abolfathi, S. 2016. Nearshore mixing due to the effects of waves and currents. PhD thesis, University of Warwick.

Abolfathi, S., and J. M. Pearson. 2017. Application of smoothed particle hydrodynamics (SPH) in nearshore mixing: a comparison to laboratory data. *Proceedings of Coastal Engineering*, https://doi.org/10.9753/icce.v35.currents.16.

Abolfathi, S., S. Dong, S. Borzooei, A. Yeganeh-Bakhtiari, and J.M. Pearson. 2018. Application of Smoothed Particle Hydrodynamics in Evaluating the Performance of Coastal Retrofits Structures, Coastal Engineering Proceedings, 1(36). https://doi.org/10.9753/icce.v36.papers.109.

Cook, S., H. L. Chan, S. Abolfathi, G. Bending, H. Schafer, J. M. Pearson. 2020a. Longitudinal dispersion of microplastics in aquatic flows using fluorometric techniques, Water Research, 115337. https://doi.org/10.1016/j.watres.2019.115337.

Cook, S., O. Price, A. King, C. Finnegan, R. van Egmond, H. Schafer, J. M. Pearson, S. Abolfathi, G. Bending. 2020b. Bedform characteristics and biofilm community development interact to modify hyporheic exchange. Science of the Total Environment, Vol. 749, 141397, Elsevier, https://doi.org/10.1016/j.scitotenv.2020.141397

Dong, S, S. Abolfathi, M. Salauddin, Z. H. Tan, J. M. Pearson. 2020. Enhancing climate resilience of vertical seawall with retrofitting – A physical modelling study. Applied Ocean Research. Volume 103, 102331. https://doi.org/10.1016/j.apor.2020.102331

Dong, S., M. Salauddin, S. Abolfathi, Z.H. Tan, and J.M. Pearson. 2018. The Influence of Geometrical Shape Changes on Wave Overtopping: A Laboratory and SPH Numerical Study, *Proceedings of Coasts, Marine Structures and Breakwaters Conference 2017*, pp. 1217-1226. https://doi.org/10.1680/cmsb.63174.1217

Fischer, H., J. List, C. Koh et al., 1979. Mixing in inland and coastal waters. Academic Press. ISBN 9780080511771.

Fitri, A., R. Hashim, S. Abolfathi, K. N. Abdul Maulud. 2019. Dynamics of sediment transport and erosion-deposition patterns in the locality of a detached low-crested breakwater on a cohesive coast. Water, 11 (8). 1721. DOI: https://doi.org/10.3390/w11081721

Goodarzi, D., K. Sookhak Lari, E. Khavasi, S. Abolfathi. 2020a. Large eddy simulation of turbidity currents in a narrow channel with different obstacle configurations. Scientific Reports, Nature Publisher Group, Vol. 10, issue 1, page 1-16. 12814, https://doi.org/10.1038/s41598-020-68830-5

Goodarzi, D., S. Abolfathi, S. Borzooei. 2020b. Modelling solute transport in water disinfection systems: effects of temperature gradient on the hydraulic and disinfection efficiency of serpentine chlorine contact tanks. Journal of Water Process Engineering, 37. 101411. https://doi.org/10.1016/j.jwpe.2020.101411

Jambeck, J.R., R. Geyer, C. Wilcox, T.R. Siegler, M. Perryman, A. Andrady, R. Narayan, and K.L Law. 2015. Plastic waste inputs from land into the ocean. Science, 347(6223), 768-771.

Karakolis, E.G., B. Nguyen, J.B. You, C.M. Rochman, D. Sinton. 2019. Fluorescent dyes for visualizing microplastic particles and fibers in laboratory-based studies. Environ. Sci. Technol. Lett., 6 (6), pp. 334-340.

Karambas, T. V. 1999. Mixing in the surfzone: A theoretical approach. Coastal Engineering, 18, 1-19.

Lebreton, L.C.M., J. van der Zwet, J.W. Damsteeg, B. Slat, A. Andrady, J. Reisser. 2017. River plastic emissions to the world's oceans. Nature Communication, 8, Article 15611.

Mansard E. P. D., and E. R. Funke. 1980. The measurement of incident and reflected spectra using least squares method. 17th International Conference on Coastal Engineering.

Salauddin, M., J. J. O'Sullivan, S. Abolfathi, J. M. Pearson. 2020. Extreme Wave Overtopping at Ecologically Modified Sea Defences. EGU General Assembly, 6162. https://doi.org/10.5194/egusphere-egu2020-6162, 2020.

Seidensticker, S., P. Grathwohl, J. Lamprecht, et al. 2018. A combined experimental and modeling study to evaluate pH-dependent sorption of polar and non-polar compounds to polyethylene and polystyrene microplastics. Environ Sci Eur 30, 30. https://doi.org/10.1186/s12302-018-0155-z

Taylor, G. I. 1954. The dispersion of matter in a turbulent flow through a pipe. *Proceedings of Royal Society*. *London*. Ser. A, 223, 446-468.

Wright, S. L., & Kelly, F. J. 2017. Plastic and Human Health: A micro Issue? Environmental Science & Technology, 6634-6647.

Yeganeh-Bakhtiary, A., H. Houshangi, S. Abolfathi. 2020. Lagrangian two-phase flow modeling of scour in front of vertical breakwater. Coastal Engineering Journal, 62:2, 252-266, DOI: 10.1080/21664250.2020.1747140.

Yeganeh-Bakhtiary, A., H. Houshangi, F. Hajivalie, and S. Abolfathi. 2017. A Numerical Study on Hydrodynamics of Standing Waves in Front of Caisson Breakwaters with WCSPH Model, Coastal Engineering Journal, 59:1, 1750005-1-1750005-31, DOI: 10.1142/S057856341750005X